Experimental and Numerical Studies on Nonlinear Dynamic Behavior of Rotor System Supported by Ball Bearings

Changqing Bai
School of Aerospace,
Xi'an Jiaotong University,
Xi'an 710049, China
e-mail: baichq@mail.xjtu.edu.cn

Hongyan Zhang
School of Science,
Chang'an University,
Xi'an 710064, China

Qingyu Xu
School of Aerospace,
Xi'an Jiaotong University,
Xi'an 710049, China

Ball bearings are important mechanical components in high-speed turbomachinery that is liable for severe vibration and noise due to the inherent nonlinearity of ball bearings. Using experiments and the numerical approach, the nonlinear dynamic behavior of a flexible rotor supported by ball bearings is investigated in this paper. An experimental ball bearing-rotor test rig is presented in order to investigate the nonlinear dynamic performance of the rotor systems, as the speed is beyond the first synchroresonance frequency. The finite element method and two-degree-of-freedom dynamic model of a ball bearing are employed for modeling the flexible rotor system. The discrete model of a shaft is built with the aid of the finite element technique, and the ball bearing model includes the nonlinear effects of the Hertzian contact force, bearing internal clearance, and so on. The nonlinear unbalance response is observed by experimental and numerical analysis. All of the predicted results are in good agreement with experimental data, thus validating the proposed model. Numerical and experimental results show that the resonance frequency is provoked when the speed is about twice the synchroresonance frequency, while the subharmonic resonance occurs due to the nonlinearity of ball bearings and causes severe vibration and strong noise. The results show that the effect of a ball bearing on the dynamic behavior is noticeable in optimum design and failure diagnosis of high-speed turbomachinery. [DOI: 10.1115/1.4000586]

Keywords: *ball bearing, rotor, experiment, nonlinear vibration*

1 Introduction

Ball bearings are one of the essential and important components in sophisticated turbomachinery such as rocket turbopumps, aircraft jet engines, and so on. Because of the requirement of acquiring higher performance in the design and operation of ball bearings-rotor systems, accurate predictions of vibration characteristics of the systems, especially in the high rotational speed condition, have become increasingly important.

Inherent nonlinearity of ball bearings is due to Hertzian contact forces and the internal clearance between the ball and the ring. Many researchers have devoted themselves to investigating the dynamic characteristics associated with ball bearings. Gustafsson et al. [1] studied the vibrations due to the varying compliance of ball bearings. Saito [2] investigated the effect of radial clearance in an unbalanced Jeffcott rotor supported by ball bearings using the numerical harmonic balance technique. Aktürk et al. [3] used a three-degree-of-freedom system to explore the radial and axial vibrations of a rigid shaft supported by a pair of angular contact ball bearings. Liew et al. [4] summarized four different dynamic models of ball bearings, viz., two or five degrees of freedom, with or without ball centrifugal force, which could be applied to determine the vibration response of ball bearing-rotor systems. Bai and Xu [5] presented a general dynamic model to predict dynamic properties of rotor systems supported by ball bearings. De Mul et al. [6] presented a five-degree-of-freedom (5DOF) model for the calculation of the equilibrium and associated load distribution in ball bearings. Mevel and Guyader [7] described different routes to chaos by varying a control parameter. Jang and Jeong [8] proposed an excitation model of ball bearing waviness to investigate the bearing vibration. Then, considering the centrifugal force and gyroscopic moment of ball, they developed an analytical method to calculate the characteristics of the ball bearing under the effect of waviness in Ref. [9]. Tiwari et al. [10,11] employed a two-degree-of-freedom model to analyze the nonlinear behaviors and stability associated with the internal clearance of a ball bearing. Harsha [12–14], taking into account different sources of nonlinearity, investigated the nonlinear dynamic behavior of ball bearing-rotor systems. Gupta et al. [15] studied the nonlinear dynamic response of an unbalanced horizontal flexible rotor supported by a ball bearing. With the aid of the Floquet theory, Bai et al. [16] investigated the effects of axial preload on nonlinear dynamic characteristics of a flexible rotor supported by angular contact ball bearings. Using the harmonic balance method, Sinou [17] performed a numerical analysis to investigate the nonlinear unbalance response of a flexible rotor supported by ball bearings.

In the abovementioned studies, main attention has been paid to the ball bearing modeling and the dynamic properties analysis according to simple bearing-rotor models. With theoretical analysis and experiment, Yamamoto et al. [18] studied a nonlinear forced oscillation at a major critical speed in a rotating shaft, which was supported by ball bearings with angular clearances. Ishida and Yamamoto [19] studied the forced oscillations of a rotating shaft with nonlinear spring characteristics and internal damping. They found that a self-excited oscillation appears in the wide range above the major critical speed. A dynamic model was derived, and experiments are carried out with a laboratory test rig for studying the misaligned effect of misaligned rotor-ball bearing systems in Ref. [20]. Tiwari et al. [21] presented an experimental analysis to study the effect of radial internal clearance of a ball bearing on the bearing stiffness of a rigid horizontal rotor. These experimental results validated theoretical results reported in their

Contributed by the International Gas Turbine Institute of ASME for publication in the Journal of Engineering for Gas Turbines and Power. Manuscript received March 31, 2009; final manuscript received October 5, 2009; published online May 28, 2010. Assoc. Editor: Patrick S. Keogh.

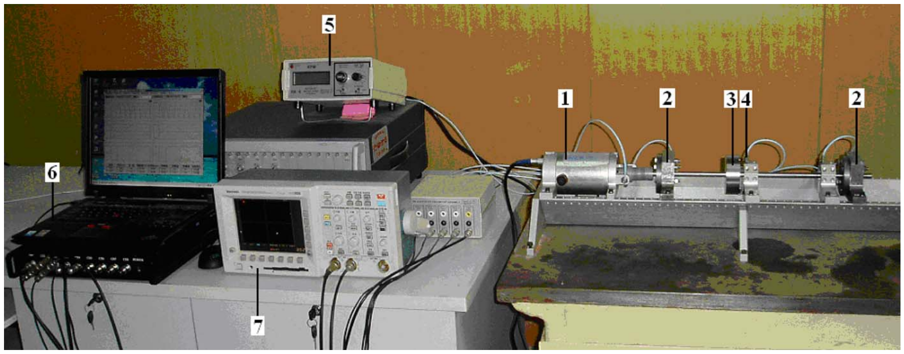

Fig. 1 Experimental rig

literatures [10,11]. Recently, Ishida et al. [22] investigated theoretically and experimentally the nonlinear forced vibrations and parametrically excited vibrations of an asymmetrical shaft supported by ball bearings. Mevel and Guyader [23] used an experimental test bench to confirm the predicted routes to chaos in their previous paper [7]. It is noticeable of lack of experiments on nonlinear dynamic behavior of flexible rotor systems supported by ball bearings. In Ref. [24], the finite element method was used to model a LH_2 turbopump rotor system supported by ball bearings. Numerical results show that the subharmonic resonance, as well as synchroresonance, occurs in the start-up process. It is found that the subharmonic resonance is an important dynamic behavior and should be considered in engineering ball bearing-rotor system design. But, the experimental and numerical studies of the subharmonic resonance in ball bearing-rotor systems are very rare.

With respect to the above, the present study is intended to cast light on the subharmonic resonance characteristics in ball bearing-rotor systems using experiments and numerical approach. An experiment on an offset-disk rotor supported by ball bearings is carried out, and the finite element method and two-degree-of-freedom model of a ball bearing are employed for modeling this rotor system. The predicted results are compared with the test data, and an investigation is conducted in the nonlinear dynamic behavior of the ball bearings-rotor system.

2 Experimental Investigation

An experimental rig is employed for studying the nonlinear dynamic behavior of ball bearing-rotor systems, as shown in Fig. 1. The horizontal shaft is supported by two ball bearings at both ends, and the disk is mounted unsymmetrically. The shaft is coupled to a motor with a flexible coupling. The motor speed is controlled with a feedback controller, which gets the signals from an eddy current probe. Four eddy current probes, whose resolution is 0.5 μm, are mounted close to the disk and bearing at the right end in the horizontal and vertical directions, respectively. The displacement signals, obtained with the help of probes, are input into an oscilloscope to describe the motion orbit, and a data acquisition and processing system were used to analyze the effects of ball bearings on the nonlinear dynamic behavior. The data acquisition and processing system utilizes a full period sampling as the data acquisition method. Its sampling rate is 500 kHz maximum, and sample size is 12 bits. The system provides eight channels for vibratory response acquisition and 1 channel for rotational speed acquisition. All channels are simultaneous.

The limitation with the presented experimental setup is that the maximum attainable speed is 12,000 rpm. The first critical speed of the rotor system falls in the speed span, as the shaft is flexible and its fist synchroresonance frequency is near 66 Hz (3960 rpm). Thus, the dynamic behavior can be studied as the speed is beyond twice the synchroresonance frequency.

3 Rotor Dynamic Model

The bearing-rotor system combines an offset-disk and two ball bearings, which support the rotor at both ends. The sketch map of the system is described in Fig. 2, where the frame *oxyz* is the inertial frame. The corresponding experiment assembly is shown in Fig. 3.

3.1 Equations of Motion. Define u_x and u_y as the transverse deflections along the *ox* and *oy* directions, and θ_x and θ_y as the corresponding bending angles in the *oxz* and *oyz* planes, respectively. When u_{1x}, u_{1y}, θ_{1x}, and θ_{1y} denote the displacements of the ball bearing center location at the left end, the complex variables u_1 and θ_1 can be assumed as

$$u_1 = u_{1x} + iu_{1y}, \quad \theta_1 = \theta_{1x} + i\theta_{1y} \tag{1}$$

Denote the displacements of the disk center by u_2 and θ_2, and the displacements of the ball bearing center location at the right end by u_3 and θ_3. Using the finite element method, the equations of motion for the rotor system can be written as [25,26]

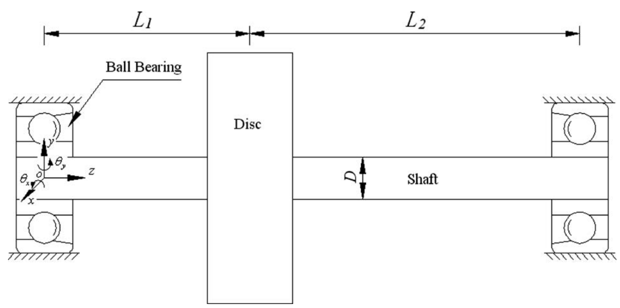

Fig. 2 Sketch map of ball bearing-rotor system

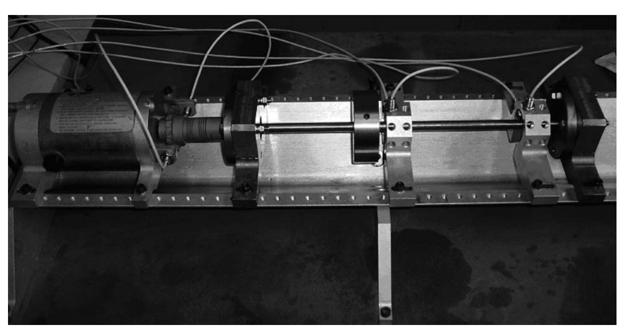

Fig. 3 Experiment assembly of ball bearing-rotor system

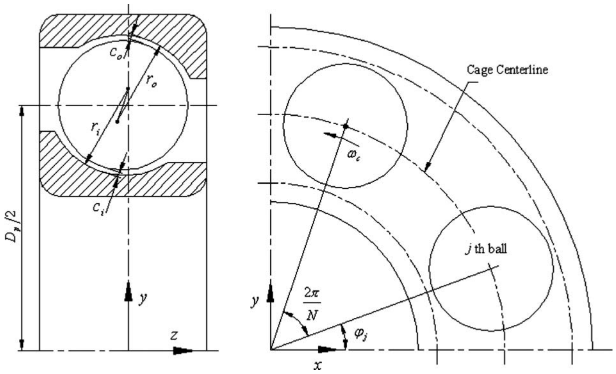

Fig. 4 Geometry in ball bearing

$$[M]\{\ddot{u}\} + ([C] - \omega[G])\{\dot{u}\} + [K]\{u\} = \{F_g\} + \{F_u(t)\} + \{F_b(u,t)\} \quad (2)$$

where $[M]$, $[C]$, $[K]$, and $[G]$ are the mass, damping, stiffness, and gyroscopic matrix of the rotor system, respectively, ω is the rotational speed, and $\{u\}$ is the displacement vector

$$\{u\} = \{u_1 \quad \theta_1 \quad u_2 \quad \theta_2 \quad u_3 \quad \theta_3\}^T \quad (3)$$

$\{F_g\}$ and $\{F_u\}$ are the vectors of gravity load and unbalance forces. $\{F_b\}$ is the vector of nonlinear forces associated with ball bearings.

$$\{F_b\} = \{f_b(u_1,t) \quad 0 \quad 0 \quad 0 \quad f_b(u_3,t) \quad 0\}^T \quad (4)$$

where f_b is the nonlinear restoring force of the ball bearing.

3.2 Ball Bearing Forces. A ball bearing is depicted in a frame of axes $oxyz$ in Fig. 4. The contact deformation for the j-th rolling element δ_j is given as

$$\delta_j = u_{bx} \cos \varphi_j + u_{by} \sin \varphi_j - c_i - c_o \quad (5)$$

where c_i and c_o are the internal radial clearance between the inner, outer race, and rolling elements, respectively, in the direction of contact, and u_{bx} and u_{by} are the relative displacements of the inner and outer race along the x and y directions, respectively. As shown in Fig. 4, the angular location of the j-th rolling element φ_j can be obtained from

$$\varphi_j = \frac{2\pi(j-1)}{N} + \omega_c t + \varphi_0 \quad (6)$$

where N, ω_c, t, and φ_0 are the number of rolling elements, cage angular velocity, time, and initial angular location, respectively. The cage angular velocity can be expressed as [27]

$$\omega_c = \frac{1}{2}\omega\left[1 - \frac{D_b}{D_p}\cos \alpha\right] \quad (7)$$

where D_b and D_p are the ball diameter and bearing pitch diameter, respectively. α is the contact angle, which is concerned with the clearance and can be obtained as follows:

$$\alpha = \arccos\left(1 - \frac{c_i + c_o}{r_i + r_o - D_b}\right) \quad (8)$$

Referring to Fig. 4, r_i and r_o are the inner and outer groove radius, respectively.

If the contact deformation δ_j is positive, the contact force could be calculated using the Hertzian contact theory; otherwise, no load is transmitted. The contact force Q_j between the j-th ball and race can be expressed as follows:

$$Q_j = \begin{cases} k_b \delta_j^{3/2} & \delta_j > 0 \\ 0 & \delta_j < 0 \end{cases} \quad (9)$$

where k_b is the contact stiffness that can be given by

Table 1 Angular contact ball bearing 7200AC parameters

Bearing parameters	Value
Number of balls (N)	9
Ball diameter (D_b)	4.74 mm
Pitch diameter (D_p)	20.45 mm
Inner race curvature radius (r_i)[a]	2.5596mm
Outer race curvature radius (r_o)[a]	2.4648mm
Inner race clearance (c_i)	0.001 mm
Outer race clearance (c_o)	0.002 mm

[a]Estimated value.

$$k_b = \left[\frac{1}{(1/k_{bi})^{2/3} + (1/k_{bo})^{2/3}}\right]^{3/2} \quad (10)$$

where k_{bi} and k_{bo} are the load-deflection constants between the inner and outer ball race, respectively [28].

Summing the contact forces for each rolling element, the total bearing reaction f_b in a complex form is

$$f_b = \sum_{j=1}^{N} Q_j(\cos \varphi_j + i \sin \varphi_j) \quad (11)$$

4 Experimental and Numerical Analysis

As shown in Fig. 2, the experimental assembly and the finite element model used in the dynamic analysis represent the ball bearing-rotor system with the following geometrical properties: length between the disk center and left end bearing center $L_1 = 120$ mm; length between the disk center and right end bearing center $L_2 = 230$ mm; and the shaft diameter $D = 10$ mm. In addition, the elastic shaft material is steel of density $\rho = 7950$ kg/m^3, Young's modulus $E = 211$ GPa, and Poisson's ratio $\upsilon = 0.3$. The ball bearings at both ends are the same model, 7200AC, and its parameters are listed in Table 1.

The unbalance load is acted with the aid of the mass fixed on the disk. By virtue of this act, the mass eccentricity of the disk can be definitely ascertained. As the mass eccentricity of the disk is 0.032 mm, the vibratory response at different rotational speed is determined via a numerical integration and Newton–Raphson iterations of the nonlinear differential equation (2). Note that the clearances used to simulate the bearings are measured ones. The horizontal and vertical displacements signals near the disk are acquired at different times, along with the increased rotational speed. Thus, the amplitudes of vibration at different speeds are determined according to the test data, and overall amplitudes are illustrated in Fig. 5, as the rotor system is run from $\omega = 2000$ rpm to 10,000 rpm. The prediction results compared with experimental data are shown in Fig. 5. It can be found that all of the predicted results are in good agreement with experimental data, thus validating the proposed model. The first predicted resonance peak—the so called forward critical speed in linear theory, located at $\omega = 3960$ rpm, matches the experimental date near $\omega = 3900$ rpm quite well. Moreover, the other amplitude peak appearing in the rotational speed range $\omega = 7700$ rpm to 8100 rpm can be found in both experimental and numerical analysis results. The corresponding frequency value of this peak is just the frequency doubling of the system critical speed.

The Floquet theory can be used for analyzing the stability and topological properties of the periodic solution of the ball bearing-rotor system. If the gained Floquet multipliers are less than unity, the periodic solution of the system is stable. If at least one Floquet multiplier exists with the absolute value higher than unity, the periodic solution is unstable and the topological properties of response alter into nonperiodic motion [29]. The leading Floquet multipliers and its absolute value at $\omega = 7600$ rpm, 8029 rpm, and 8200 rpm are shown in Table 2. It is found that the leading Flo-

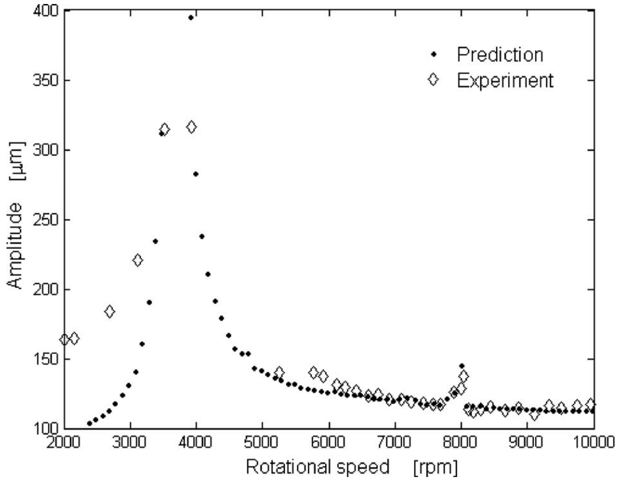

Fig. 5 Amplitude of u_{2y} versus rotational speed comparisons for prediction and experiment

quet multiplier of the system remains in the unit circle, which indicates a synchronous response, as the rotational speed is less than 7700 rpm. Stability analysis shows that the imaginary parts of the two leading Floquet multipliers move in opposite directions along the real axis near $\omega=7700$ rpm. When the speed exceeded $\omega=7700$ rpm, the leading Floquet multiplier crosses the unit circle through -1, as shown in Table 2. The periodic solution loses stability and undergoes a period-doubling bifurcation to a period-2 response, which indicates that a subharmonic resonance occurs. The subharmonic resonance keeps on from $\omega=7700$ rpm to 8100 rpm. At $\omega=8100$ rpm, the leading Floquet multiplier moves inside the unit circle through -1. Imply that the subharmonic resonance vanishes and the synchronous response returns. The synchronous response then continues to exist for speeds above $\omega=8100$ rpm.

The waterfall map of frequency spectrums comparisons for prediction and experiment results are illustrated in Fig. 6. It can be found that agreement between the prediction and the experimental data is remarkable. The frequency component 66.9 Hz, near the forward resonance frequency, emerges and its amplitude rises significant when the rotational speed is near 8029 rpm. It is shown that the resonance frequency is provoked when the speed is about twice the critical speed of the ball bearing-rotor system, and the subharmonic resonance occurs. The experimental and numerical analysis indicate that the representative nonlinear behavior and the subharmonic resonance arise from the nonlinearity of ball bearings, Hertzian contact forces, and internal clearance.

The orbit and frequency spectrum at $\omega=8029$ rpm are plotted in Fig. 7. Not only the prediction orbit but also the experiment results imply that the response is a period-2 motion, which is illustrated in Fig. 7(*a*). The predicted frequency components, consisting of $\omega=133.8$ Hz (8029 rpm) and $\omega/2=66.9$ Hz (4014 rpm), coincide with experimental data. It indicates that the periodic response loses stability through a period-doubling bifurcation to a period-2 response. Thus, the subharmonic resonance occurs

Table 2 Floquet multiplier of the ball bearing-rotor system

Rotational speed (rpm)	Leading Floquet multiplier	Absolute value of leading Floquet multiplier
7600	$-0.0862+0.9824i$	0.9862
	$-0.0862-0.9824i$	0.9862
8029	-1.0736	1.0736
8200	$-0.0952+0.9770i$	0.9816
	$-0.0952-0.9770i$	0.9816

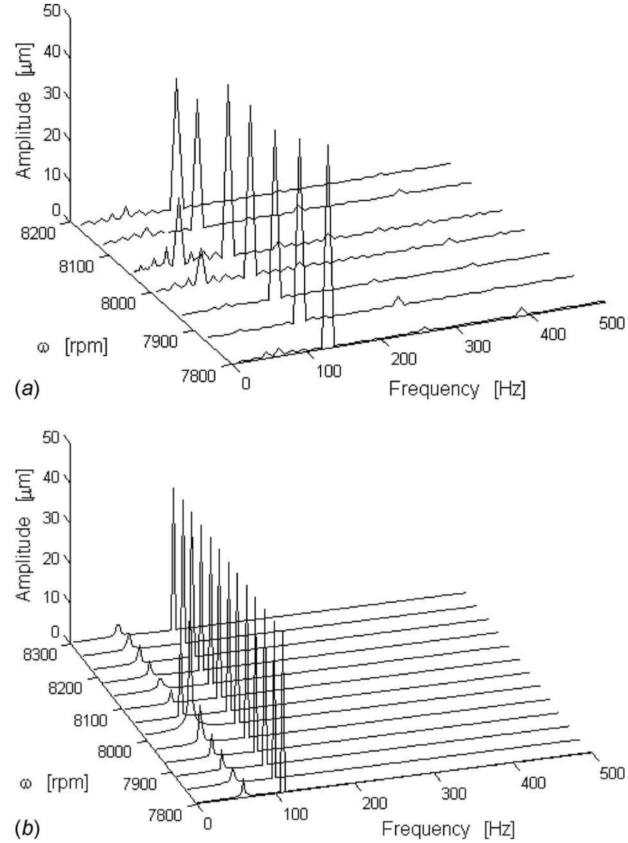

Fig. 6 Waterfall map of frequency spectrums at different rotational speed; (*a*) experiment data and (*b*) numerical analysis results

due to the effects of ball bearings. It can cause severe vibration and strong noise. Moreover, the subharmonic resonance could couple with other destabilizing effects on engineering rotor systems such as Alford forces, internal damping, and so on, and induce the rotor to lose stability and damage.

5 Conclusions

An experimental rig is employed to investigate the nonlinear dynamic behavior of ball bearing-rotor systems. The corresponding dynamic model is established with the finite element method and 2DOF dynamic model of a ball bearing, which includes the nonlinear effects of the Hertzian contact force and bearing internal clearance. All of the predicted results are in good agreement with experimental data, thus validating the proposed model.

Numerical and experimental results show that the resonance frequency is provoked, and the subharmonic resonance occurs due to the nonlinearity of ball bearings when the speed is about twice the synchroresonance frequency. The subharmonic resonance cannot only cause severe vibration and strong noise, but also induce the rotor to lose stability and damage, once coupled with other destabilizing effects on high-speed turbomachinery such as Alford forces, internal damping, and so on. It is found that the effect of the Hertzian contact forces could also induce a subharmonic resonance, even if the internal clearance was not present. But, the response amplitude and subharmonic component of the rotor system without internal clearance are less than that with both Hertzian contact forces and internal clearance. Otherwise, the clearance may be unavoidable under high-speed operations, where the bearings are axially preloaded since the effect of unbalanced load is significant at high speed. Thus, the nonlinearity of ball bearings,

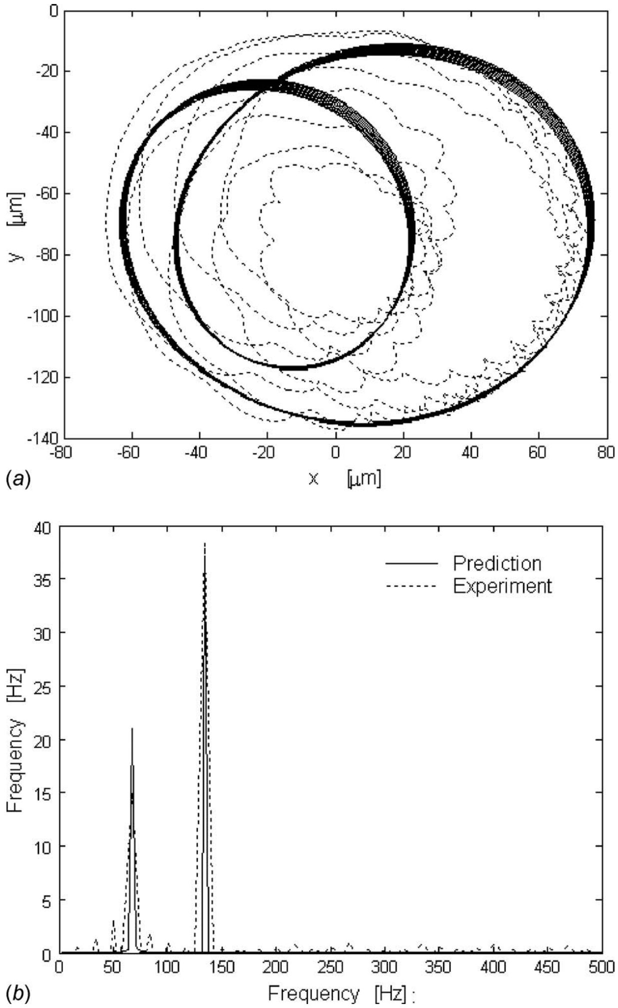

Fig. 7 Comparisons for prediction and experiment at 8029 rpm; (*a*) orbit and (*b*) amplitude spectrums of disk center displacement in vertical direction

Hertzian contact forces, and internal clearance should be taken into account in ball bearing-rotor system design and failure diagnosis.

Acknowledgment

The authors would like to acknowledgment the support of the National Natural Science Foundation of China (Grant No. 10902080) and Natural Science Foundation of Shaanxi Province (Grant Nos. SJ08A19 and 2009JQ1008).

References

[1] Gutafsson, O., and Tallian, T., 1963, "Research Report on Study of the Vibration Characteristics of Bearings," SKF Ind. Inc. Technical Report No. AL631023.
[2] Saito, S., 1985, "Calculation of Non-Linear Unbalance Response of Horizontal Jeffcott Rotors Supported by Ball Bearings With Radial Clearances," ASME J. Vib., Acoust., Stress, Reliab. Des., **107**(4), pp. 416–420.
[3] Aktürk, N., Uneeb, M., and Gohar, R., 1997, "The Effects of Number of Balls and Preload on Vibrations Associated With Ball Bearings," ASME J. Tribol., **119**, pp. 747–753.
[4] Liew, A., Feng, N., and Hahn, E., 2002, "Transient Rotordynamic Modeling of Rolling Element Bearing Systems," ASME J. Eng. Gas Turbines Power, **124**(4), pp. 984–991.
[5] Bai, C. Q., and Xu, Q. Y., 2006, "Dynamic Model of Ball Bearing With Internal Clearance and Waviness," J. Sound Vib., **294**(1–2), pp. 23–48.
[6] De Mul, J. M., Vree, J. M., and Maas, D. A., 1989, "Equilibrium and Associated Load Distribution in Ball and Roller Bearings Loaded in Five Degrees of Freedom While Neglecting Friction—Part I: General Theory and Application to Ball Bearings," ASME J. Tribol., **111**, pp. 142–148.
[7] Mevel, B., and Guyader, J. L., 1993, "Routes to Chaos in Ball Bearings," J. Sound Vib., **162**, pp. 471–487.
[8] Jang, G. H., and Jeong, S. W., 2002, "Nonlinear Excitation Model of Ball Bearing Waviness in a Rigid Rotor Supported by Two or More Ball Bearings Considering Five Degrees of Freedom," ASME J. Tribol., **124**, pp. 82–90.
[9] Jang, G. H., and Jeong, S. W., 2003, "Analysis of a Ball Bearing With Waviness Considering the Centrifugal Force and Gyroscopic Moment of the Ball," ASME J. Tribol., **125**, pp. 487–498.
[10] Tiwari, M., Gupta, K., and Prakash, O., 2000, "Effect of Radial Internal Clearance of a Ball Bearing on the Dynamics of a Balanced Horizontal Rotor," J. Sound Vib., **238**(5), pp. 723–756.
[11] Tiwari, M., Gupta, K., and Prakash, O., 2000, "Dynamic Response of an Unbalanced Rotor Supported on Ball Bearings," J. Sound Vib., **238**(5), pp. 757–779.
[12] Harsha, S. P., 2005, "Non-Linear Dynamic Response of a Balanced Rotor Supported on Rolling Element Bearings," Mech. Syst. Signal Process., **19**(3), pp. 551–578.
[13] Harsha, S. P., 2006, "Rolling Bearing Vibrations—The Effects of Surface Waviness and Radial Internal Clearance," Int. J. Computational Methods in Eng Sci. and Mech., **7**(2), pp. 91–111.
[14] Harsha, S. P., 2006, "Nonlinear Dynamic Analysis of a High-Speed Rotor Supported by Rolling Element Bearings," J. Sound Vib., **290**(1–2), pp. 65–100.
[15] Gupta, T. C., Gupta, K., and Sehqal, D. K., 2008, "Nonlinear Vibration Analysis of an Unbalanced Flexible Rotor Supported by Ball Bearings With Radial Internal Clearance," *Proceedings of the ASME Turbo Expo*, Vol. 5, pp. 1289–1298.
[16] Bai, C. Q., Zhang, H. Y., and Xu, Q. Y., 2008, "Effects of Axial Preload of Ball Bearing on the Nonlinear Dynamic Characteristics of a Rotor-Bearing System," Nonlinear Dyn., **53**(3), pp. 173–190.
[17] Sinou, J. J., 2009, "Non-Linear Dynamics and Contacts of an Unbalanced Flexible Rotor Supported on Ball Bearings," Mech. Mach. Theory, **44**(9), pp. 1713–1732.
[18] Yamamoto, T., Ishida, Y., and Ikeda, T., 1984, "Vibrations of a Rotating Shaft With Rotating Nonlinear Restoring Forces at the Major Critical Speed," Bull. JSME, **27**(230), pp. 1728–1736.
[19] Ishida, Y., and Yamamoto, T., 1993, "Forced Oscillations of a Rotating Shaft With Nonlinear Spring Characteristics and Internal Damping (1/2 Order Subharmonic Oscillations and Entrainment)," Nonlinear Dyn., **4**(5), pp. 413–431.
[20] Lee, Y. S., and Lee, C. W., 1999, "Modeling and Vibration Analysis of Misaligned Rotor-Ball Bearing Systems," J. Sound Vib., **224**(1), pp. 17–32.
[21] Tiwari, M., Gupta, K., and Prakash, O., 2002, "Experimental Study of a Rotor Supported by Deep Groove Ball Bearing," Int. J. Rotating Mach., **8**(4), pp. 243–258.
[22] Ishida, Y., Liu, J., Inoue, T., and Suzuki, A., 2008, "Vibrations of an Asymmetrical Shaft With Gravity and Nonlinear Spring Characteristics (Isolated Resonances and Internal Resonances)," ASME J. Vib. Acoust., **130**(4), p. 041004.
[23] Mevel, B., and Guyader, J. L., 2008, "Experiments on Routes to Chaos in Ball Bearings," J. Sound Vib., **318**, pp. 549–564.
[24] Bai, C. Q., Xu, Q. Y., and Zhang, X. L., 2006, "Dynamic Properties Analysis of Ball Bearings—Liquid Hydrogen Turbopump Used in Rocket Engine," ACTA Aeronaut. Astronaut. Sinica, **27**(2), pp. 258–261.
[25] Nelson, H., 1980, "A Finite Rotating Shaft Element Using Timoshenko Beam Theory," ASME J. Mech. Des., **102**(4), pp. 793–803.
[26] Zhang, W., 1999, *Basis of Rotordynamic Theory*, Science Press, Beijing, China, Chap. 3.
[27] Harris, T. A., 1984, *Rolling Bearing Analysis*, 2nd ed., Wiley, New York.
[28] Aktürk, N., 1993, "Dynamics of a Rigid Shaft Supported by Angular Contact Ball Bearings," Ph.D. thesis, Imperial College of Science, Technology and Medicine, London, UK.
[29] Zhou, J. Q., and Zhu, Y. Y., 1998, *Nonlinear Vibrations*, Xi'an Jioatong University Press, Xi'an, China.